2021 IEEE/ASME International Conference on
Advanced Intelligent Mechatronics (AIM)

Incorporating Observability via Control Barrier Functions with Application to Range-based Target Tracking

Demetris Coleman, Shaunak D. Bopardikar, and Xiaobo Tan

***Abstract*—In nonlinear systems, the control input often directly impacts observability of the system. In this paper, we investigate the use of control barrier functions (CBFs) for enforcing observability of a mobile robot in target tracking, when only the distance to the target is measured. The problem is motivated by practical applications for autonomous robots when operating in GPS-denied environments. To address the tradeoffs between localization accuracy and tracking performance, a tracking controller is augmented by a control barrier function based on an observability metric. Two examples are used to show the efficacy of the approach, one with unicycle dynamics on a plane, and the other based on gliding robotic fish with complex 3D dynamics. The approach taken in this work is compared to a model predictive controller that optimizes a joint cost function of tracking error and observability metric. While both approaches are shown to maintain observability and enable tracking, the CBF-based approach is shown to have several advantages.**

I. Introduction

It is often possible to obtain measurements of distance to a beacon or another robot using the hardware embedded in the communication systems of the robots. This is a useful feature for autonomous robots operating in GPS-denied environments. Autonomous underwater vehicles (AUVs), which have become valuable for a myriad of applications [1], [2], are one such class of robots that regularly operate in GPS-denied environments. The inability to take advantage of radio frequency-based solutions to localization, navigation, and communication makes these tasks considerably more difficult for AUVs. In addition, techniques like simultaneous localization and mapping are not always applicable due to the lack of sufficient number of landmarks.

Several approaches to localization and navigation have been developed for underwater environments [3]. One such approach involves acoustic modems, such as the micromodem developed by Woods Hole Oceanographic Institute [4], to provide communication and ranging between underwater vehicles or beacons. Due to the capabilities of acoustic modems, many researchers began a general study of using static beacons or surface vehicles as communication and navigation aids (CNAs) to underwater vehicles [5]–[10]. The single beacon navigation (SBN) problem and its variants are a particularly interesting instance of this class of problems. In the SBN problem, an AUV estimates its position using inertial sensors, the knowledge of its dynamic model, and the measurement of its range to a single beacon while locomoting.

The observability of the SBN problem has been heavily studied in literature. The authors of [11] studied the observability of SBN with the kinematic model of an AUV moving in the horizontal plane and gave an explanation of when the position of the vehicle can be found using only measurements of distance from a static beacon. The authors of [12] investigated the observability of relative localization of two AUVs equipped with velocity, depth, and range measurement sensors. They proposed an observability metric, derived an expression for it, and showed that the degradation of localization performance depends on the range between the vehicles and the angle between the relative velocity and position vectors. The condition number of the empirical observability Gramian has been used in path planning to improve observability of a uniform flow field in [13]. Relative pose estimation based on range measurements between two robots moving in a 3D environment is explored in [14], but only the kinematic model is considered. In [15], the authors argued that optimizing measures of the observability Gramian as a surrogate for the estimation performance may provide irrelevant or misleading trajectories for planning under observation uncertainty. They instead suggested using measures of the Posterior Fisher Information Matrix. As an example, they used the trace of the covariance matrix produced by a Kalman filter as a metric to improve observability while path planning.

Most of these works focus on localization, navigation, or path planning. Control based on observability metrics in the context of range measurement is relatively less explored. The authors of [16] developed a controller for homing in on a static beacon using range measurements. The controller was inspired by previous results on observable paths, but used a heuristic approach based on a covariance threshold to achieve observable maneuvers. In [17], the authors proposed two methods for greedy-optimal steering control for CNAs. They considered the AUVs as static beacons and used approximate optimization of the condition number of the observability Gramian to steer the CNAs, thereby improving localization for underwater vehicles. In [18], a model predictive controller (MPC) is designed to optimize a weighted cost on observability metrics and tracking error to improve tracking performance for a robot unable to measure its position.

Like [18], this work studies the application of observability-based control to the target tracking problem. It differentiates itself from existing work by taking a constraint-based approach and enforcing observability through control barrier functions (CBFs). In recent years, CBFs have been heavily studied

The work was supported in part by National Science Foundation (IIS 1848945, ECCS 2030556) and Department of Education (Grant # P200A180025).

Demetris Coleman Shaunak Bopardikar, and Xiaobo Tan are with the Department of Electrical and Computer Engineering, Michigan State University, East Lansing, MI 48824, USA. Email: colem404@msu.edu (D.C.), shaunak@egr.msu.edu (S.B), xbtan@egr.msu.edu (X.T)

in the context of safety-critical controllers [19]–[22]. Some works also leverage CBFs to facilitate multi-objective control in multi-robot systems [23]–[26]. CBFs enforce forward invariance of a set with respect to the state of a dynamical system, and thereby, ensure safety properties [19]. This particular ability is shown to work with any locally Lipschitz controller for control affine systems through a computationally efficient optimization scheme. The ease of computation and theoretical guarantees for forward invariance makes this approach an attractive solution for improving observability when tracking with only range measurements. In contrast, adding optimization of the observability metrics to the finite horizon MPC cost function causes the problem to quickly become infeasible for real-time operation of complex systems. In addition, the weight that balances observability and control performance in the MPC approach has to be carefully selected in order to obtain acceptable performance. We circumvent the computational complexity and manual tuning by enforcing the forward invariance of an observable set through the CBF constraint at every instant.

The rest of this paper is organized as follows. Section II reviews some concepts of observability and control barrier functions. Section III discusses the proposed approach. Analysis for two example systems and simulation results are presented in Section IV followed by concluding remarks in Section V.

II. Background Material

In this section, we briefly review the concepts of the nonlinear observability rank condition and control barrier functions.

A. Nonlinear Observability Rank Condition

Given a general nonlinear system modeled by

$$\begin{cases} \dot{x} = f(x,u) \\ y = h(x), \end{cases} \tag{1}$$

with state $x \in R^n$, input $u \in R^i$, and output $y \in R^o$, its observability can be studied using the concept of local weak observability introduced in [27]. By defining the Lie derivatives of the output vector $h(x)$ as

$$\begin{aligned} \mathcal{L}_f^0 h &= h, \\ \mathcal{L}_f^1 h &= \nabla_x h f, \\ \mathcal{L}_f^2 h &= \nabla_x [\mathcal{L}_f^1 h] f, \\ \mathcal{L}_f^l h &= \nabla_x [\mathcal{L}_f^{l-1} h] f, \end{aligned} \tag{2}$$

and the nonlinear observability matrix for the system in Eq. (1), evaluated at $x = x_1$, can be constructed as

$$\mathcal{O}(x_1) = \begin{bmatrix} \nabla_x \mathcal{L}_f^0 h(x_1) \\ \nabla_x \mathcal{L}_f^1 h(x_1) \\ \vdots \\ \nabla_x \mathcal{L}_f^l h(x_1) \end{bmatrix}, \tag{3}$$

where l is a positive integer index. The observability rank condition for nonlinear systems states that system (1) is *locally weakly observable* at x_1 if there exists an input, u, such that the resulting matrix $\mathcal{O}(x_1)$ is full rank.

B. Control Barrier Functions

Consider a general nonlinear control system

$$\dot{x} = f(x) \tag{4}$$

with a Lipschitz function $f(\cdot)$ and a set $\mathcal{C}$ given by

$$\begin{aligned} \mathcal{C} &= \{x \in D \subset R^n : B(x) \geq 0\}, \\ \partial\mathcal{C} &= \{x \in D \subset R^n : B(x) = 0\}, \\ \mathrm{Int}(\mathcal{C}) &= \{x \in D \subset R^n : B(x) > 0\}, \end{aligned} \tag{5}$$

for a smooth function $B(x) : R^n \to R$. The set $\mathcal{C}$ is called forward invariant with respect to (4) if the initial condition $x_0 = x(0) \in \mathcal{C}$ implies that $x(t) \in \mathcal{C}, \forall t > 0$. If there exists an extended class $\mathcal{K}_\infty$ function $\alpha : (-a, b) \to (-\infty, \infty)$ with $a, b > 0$ and a set D with $\mathcal{C} \subseteq D \subset R^n$ such that

$$\mathcal{L}_f B(x) \geq -\alpha(B(x)), \tag{6}$$

for all $x \in D$, then $B(x)$ is a zeroing barrier function and $\mathcal{C}$ is forward invariant with respect to the system in Eq. (4) [21].

Control barrier functions are a synthesis tool derived from barrier functions[1] and are used to enforce forward invariance of a set $\mathcal{C}$ for a control system. In the case of an affine control system

$$\dot{x} = f(x) + g(x)u \tag{7}$$

with f and g locally Lipschitz, the state $x \in D \subset R^n$, and input $u \in U \subset R^m$, if there exists an extended class $\mathcal{K}_\infty$ function α such that

$$\sup_{u \in U} [\mathcal{L}_f B(x) + \mathcal{L}_g B(x) u] \geq -\alpha(B(x)), \forall x \in D, \tag{8}$$

then, $B(x)$ is a control barrier function and the set $\mathcal{C}$ is forward invariant with respect to the system (7). This holds for any Lipschitz controller in the set

$$K_{cbf}(x) = \{u \in U : \mathcal{L}_f B(x) + \mathcal{L}_g B(x) u + \alpha(B(x)) \geq 0\}$$

where $K_{cbf}(x)$ is the set of all controls that render the set $\mathcal{C}$ forward invariant [21], [22] .

III. Proposed Approach

A. Problem Formulation

In this work, we consider the problem of target tracking given the measurement of distance from a target. The objective is to find a feedback controller that improves the observability of the tracker's location, while simultaneously achieving the goal of tracking the target's position. We assume that the target's absolute location is communicated to the tracker, a good estimate of initial relative position is given, and the range to the target is measured. We also assume that the tracker is able to measure or estimate its own full state vector with the exception of position. Given the target's position $x_{ta}(t)$, $y_{ta}(t)$

[1]Both zeroing barrier functions and the closely related reciprocal barrier functions are discussed in [21]. Here, we focus only on the zeroing barrier functions.

in real time, we desire to minimize the error between the target and tracker positions. We define

$$\tau_e(t) = \begin{bmatrix} x(t) - x_{ta}(t) \\ y(t) - y_{ta}(t) \end{bmatrix} \tag{9}$$

as the tracking error between the target and tracker positions, (x_{ta}, y_{ta}) and (x, y), and

$$\kappa_e(t) = \begin{bmatrix} x(t) - \hat{x}(t) \\ y(t) - \hat{y}(t) \end{bmatrix} \tag{10}$$

as the estimation error between the true and estimated tracker positions. The tracker is a general nonlinear agent with state X, control input U, dynamics

$$\dot{X} = f(X, U), \tag{11}$$

and a nonlinear measurement function

$$h = \begin{bmatrix} ||\tau_e|| \\ M(X) \end{bmatrix} \tag{12}$$

where $M(X)$ is the state vector with the exception of the position of the tracker. The goal now, is to minimize both the Euclidean tracking error norm $||\tau_e||$ and the estimation error norm $||\kappa_e||$.

B. Observability-Based Barrier Function

We propose to enforce observability by using a control barrier function to satisfy a constraint based on an observability metric, while achieving the tracking objective. To do this, it is useful to consider the observability of the relative kinematics for the target-tracker system in a general sense as done in [12]. Consider the evolution of the relative position, $\dot{X}_r = V_r$, where V_r is the relative velocity of the system that can be expressed as a function of the tracker state X and the target velocity, $[v_{x_{ta}}, v_{y_{ta}}]^T$. The state of the relative kinematics can be expressed as

$$\begin{bmatrix} X_r \\ V_r \end{bmatrix} = \begin{bmatrix} \begin{bmatrix} x_r \\ y_r \end{bmatrix} \\ \begin{bmatrix} v_{xr} \\ v_{yr} \end{bmatrix} \end{bmatrix} = \begin{bmatrix} x - x_{ta} \\ y - y_{ta} \\ \dot{x} - v_{x_{ta}} \\ \dot{y} - v_{y_{ta}} \end{bmatrix}. \tag{13}$$

This simplifies the analysis by allowing the study of a time-invariant system rather than a time-varying one.

We further note that studying the observability based on range squared $\frac{1}{2}||\tau_e(t)||^2$ simplifies computations while keeping the same observability properties. Writing the kinematic system as

$$\begin{cases} \dot{X}_r = V_r, \\ h = \frac{1}{2}||\tau_e(t)||^2 = \frac{1}{2}(x_r^2 + y_r^2), \end{cases} \tag{14}$$

the observability matrix becomes

$$\mathcal{O}_p = \begin{bmatrix} \nabla \mathcal{L}_f^0 h \\ \nabla \mathcal{L}_f^1 h \end{bmatrix} = \begin{bmatrix} x_r & y_r \\ v_{xr} & v_{yr} \end{bmatrix}. \tag{15}$$

A necessary and sufficient condition for $\mathcal{O}_p$ to be full rank is $\det(\mathcal{O}_p) \neq 0$. A control barrier function using this metric of observability and satisfying the conditions in Eqs. (5) can be constructed as

$$B(X_r, V_r) = \det(\mathcal{O}_p)^2 = (v_{yr} x_r - v_{xr} y_r)^2, \tag{16}$$

in a general form. Later, two specific forms will be shown for example systems.

Denoting X_c as the combined state of the target and tracker, the dynamics $f_c(X_c, U) = [v_{x_{ta}}, v_{y_{ta}}, f(X, U)]^T$ become a superset of Eq. (11) and the CBF (16) can be expressed as $B(X_c)$. The control barrier function can then be integrated with some nominal tracking controller $\hat{u}$ through the following optimization problem

$$\begin{aligned} u^* = \text{argmin}_u \quad & J(u) = ||u - \hat{u}||^2 \\ \text{subject to} \quad & \\ & \frac{dB(X_c)}{dX_c} f_c(X_c, U) + \alpha(B(X_c)) \geq 0 \\ & ||u||_\infty \leq u_{max} \end{aligned} \tag{17}$$

to enforce forward invariance on the set defined by the barrier function (16). The nominal controller can be any Lipchitz controller. In previous work on control barrier functions [19], [20], [22], quadratic programming is leveraged as an efficient solution to solve the optimization problem (17) for affine control systems which, as in Eq. (8), yield a linear constraint in the control variables.

By using the proposed observability metric from Eq. 16 as a barrier function, we enforce the observability rank condition for nonlinear systems, essentially defining an observable set. The control barrier function ensures that the system state remains in this set at all times, and the system remains observable, as long as a feasible control action exists to prevent the state from leaving the set.

IV. Simulation Study

A. Unicycle Analysis

The unicycle is a standard model used to capture the essential dynamics of various vehicles moving on a 2-D plane. It also provides simple dynamics, allowing more intuitive insight. Therefore, to show the efficacy of the proposed approach, we take the unicycle model with relative position whose state is $[x_r, y_r, \psi, v]$ and has the system model

$$\begin{cases} \dot{X} = \begin{bmatrix} v\cos(\psi) - v_{x_{ta}} \\ v\sin(\psi) - v_{y_{ta}} \\ u_2 \\ u_1 \end{bmatrix}, \\ h = \begin{bmatrix} \frac{1}{2}||\tau_e(t)||^2 \\ \psi \\ v \end{bmatrix}, \end{cases} \tag{18}$$

with control the u_1 being the acceleration and u_2 being the turn rate. Constructing the observability matrix as described in Section II-A, with terms up to $\mathcal{L}_f^1 h$, yields

$$\mathcal{O} = \begin{pmatrix} x_r & y_r & 0 & 0 \\ 0 & 0 & 1 & 0 \\ 0 & 0 & 0 & 1 \\ v\cos(\psi) - v_{x_{ta}} & v\sin(\psi) - v_{y_{ta}} & * & * \\ 0 & 0 & 0 & 0 \\ 0 & 0 & 0 & 0 \end{pmatrix} \quad (19)$$

where the asteriks represent non-zero terms that are inconsequential to the rank of $\mathcal{O}$. Only $\nabla\mathcal{L}_f^0 h$ and $\nabla\mathcal{L}_f^1 h$ are needed to construct the observability matrix in Eq. (15). Using the relative speed and position from row 1 and 4 of columns 1 and 2, $v_{xr} = v\cos(\psi) - v_{x_{ta}}$ and $v_{yr} = v\sin(\psi) - v_{y_{ta}}$. We can then construct the control barrier function in (16).

B. Unicycle Simulation

In simulation, the target is represented by a predefined time-dependent trajectory $(x_{ta}(t), y_{ta}(t))$. The range between the target and the unicycle, the unicycle velocity, and the unicycle heading are measured. The measurements are corrupted with additive, zero mean, Gaussian noises and an extended Kalman filter (EKF) is used to estimate the position. For fair comparison between the different cases, the noise distribution is held constant for each simulation by setting the random number generator. A model predictive controller predicting 1 time step of 0.2 seconds is used as the base tracking controller. The controller uses the estimated position along with the measurement of the other state variables (heading, velocity) as feedback and the tracking error norm $||\tau_e||^2$ is used as the cost function. The unicycle has a maximum magnitude of $0.3\frac{m}{s}$ for velocity v to mimic the speeds of underwater gliders, and limited turn rate u_2 of $\frac{\pi}{4}\frac{\text{rad}}{s}$.

Figure 1 shows the resultant trajectories of the MPC controller with and without the control barrier function. Under state feedback, tracking is achieved with and without the control barrier function. When the CBF is not present, the unicycle follows the target trajectory almost exactly. When the tracking controller is modified through the CBF using the formulation in Eq. (17), the unicycle produces a curvy-linear path that tightly dances around the target path. Under output feedback, tracking fails for the vanilla tracking controller, but when the CBF is added, behavior similar to the state feedback case is seen and the tracking objective is still achieved.

We quantify the performance of the controllers in terms of estimation error, tracking error, and observability by collecting the statistics over the simulated trajectory. This is shown in Table I. The max and mean Euclidean norms of the estimation error κ_e are shown to be similar for all the cases in which tracking is achieved. It is notable, that the max and mean estimation errors for the output feedback case with the CBF incorporated is lower than when using state feedback and no CBF. The mean and max tracking errors are lowest for the state feedback controller without the control barrier function, while the output feedback controller with the CBF has performance similar to that of the state feedback controller with the CBF. In order to get a measure of observability

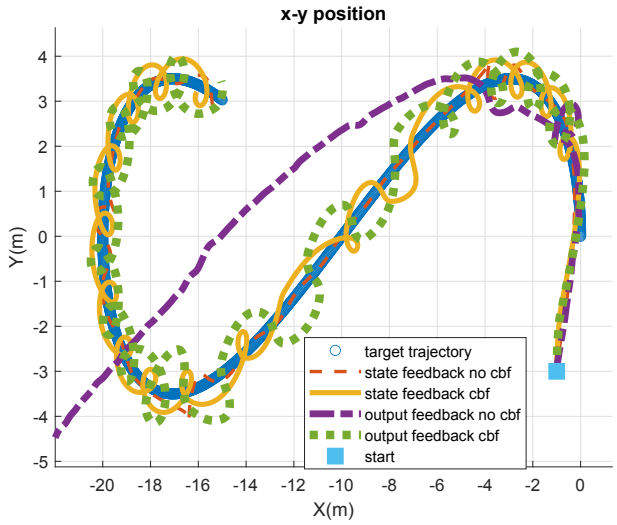

Fig. 1. Paths generated from a unicycle tracking a target moving in a figure-8 pattern using the baseline tracking controller with and without the control barrier function in the case of state and output feedback on position.

over the whole trajectory, we define the observability score as $\mathcal{O}_s = \int_0^T C^{-1} dt$, where $C^{-1} \in \{0, 1\}$ is the inverse condition number, a popular measure of observability [12], [15]. It is calculated as $C^{-1} = \frac{\min(\sigma)}{\max(\sigma)}$, the ratio of the minimum and maximum singular values σ of an observability matrix. A higher number corresponds to better observability. For the unicycle, the observability with respect to the range measurement is highest when the tracking controller is combined with the CBF. It is lowest for the tracking controller under output feedback with no CBF.

TABLE I
STATISTICS AND OBSERVABILITY SCORE FOR THE UNICYCLE MODEL SIMULATION RESULTS

CBF	no	no	yes	yes
Feedback type	state	output	state	output
max/mean $\|\|\kappa_e\|\|$ (m)	0.56/0.17	52.2/23.6	0.48/0.14	0.52/0.12
min $\|\|\tau_e\|\|$ (m)	0.0026	0.0365	0.0034	0.0317
max $\|\|\tau_e\|\|$ (m)	3.1623	34.8930	3.1623	3.1623
mean $\|\|\tau_e\|\|$ (m)	0.3506	13.4850	0.7042	0.7528
Observability score	38.48	8.51	69.56	74.59

C. Gliding Robotic Fish Analysis

Next, we study the model of a gliding robotic fish. Particulars of the robot and its dynamics are described in detail in [28], [29]. Its state vector $X = [x, y, z, v_1, v_2, v_3, \omega_1, \omega_2, \omega_3, r_{ij}]^T$, consists of the position $b_i = [x, y, z]^T$ of the robot, the 3×3 rotation matrix R from the body frame to the inertial frame with elements r_{ij}, and the body-fixed linear velocity $v_b = [v_1, v_2, v_3]^T$ and angular velocity $\omega_b = [\omega_1, \omega_2, \omega_3]^T$. After replacing the

elements of the vector b_i with the relative positions x_r, y_r, and $z_r = z$, the kinematic model is given by

$$\begin{cases} \dot{b}_i = Rv_b - [v_{x_{ta}}, v_{y_{ta}}, 0]^T, \\ \dot{R} = R\hat{\omega}_b, \end{cases} \tag{20}$$

where $\hat{\omega}_b$ is a skew symmetric matrix constructed from ω_b. The structure of the velocity dynamics is given by

$$\begin{bmatrix} \dot{v_1} \\ \dot{v_2} \\ \dot{v_3} \\ \dot{\omega_1} \\ \dot{\omega_2} \\ \dot{\omega_3} \end{bmatrix} = \begin{bmatrix} f_{v11} + a_{v1}r_{31}u_1 + f_{v12}u_3 + f_{v13}u_3^2 \\ f_{v21} + a_{v2}r_{32}u_1 + f_{v21}u_3 + f_{v22}u_3^2 \\ f_{v31} + a_{v3}r_{33}u_1 + f_{v32}u_3 + f_{v33}u_3^2 \\ f_{\omega 11} + f_{\omega 12}u_3 \\ f_{\omega 21} + a_{\omega_2}r_{33}u_2 \\ f_{\omega 31} + a_{\omega_2}r_{32}u_2 + f_{\omega 32}u_3 \end{bmatrix} \tag{21}$$

where u_i are control inputs, a_{v1}, a_{v3} and a_{ω_2} are constants, r_{vij} are elements of R, and f_{vij} and $f_{\omega ij}$ are nonlinear functions of the state vector. The measurement function in this case is $h(x) = [\frac{1}{2}||b_i||^2, z_r, v_1, v_2, v_3, \omega_1, \omega_2, \omega_3, r_{ij}]$. The observability matrix consists of the gradients of the first two Lie derivatives. As with the unicycle model, the columns associated with the measured state variables are all linearly independent and will not cause the observability matrix to lose rank, while the columns associated with the planar position are not guaranteed to have full rank. In this case, the non-zero rows can be compressed as

$$\mathcal{O}_p = \begin{bmatrix} x_r & y_r \\ \sum_{i=1}^3 r_{1i}v_i - v_{x_{ta}} & \sum_{i=1}^3 r_{2i}v_i - v_{y_{ta}} \end{bmatrix} \tag{22}$$

which reduces to a similar expression as the observability matrix $\mathcal{O}_p$ in Section III-B with $v_{xr} = \sum_{i=1}^3 r_{1i}v_i - v_{x_{ta}}$ and $v_{yr} = \sum_{i=1}^3 r_{2i}v_i - v_{y_{ta}}$.

D. Gliding Robotic Fish Simulation

TABLE II
STATISTICS AND OBSERVABILITY SCORE FOR THE GLIDING ROBOTIC FISH SIMULATION RESULTS

CBF	no	no	yes	yes
Feedback type	state	output	state	output
max/mean $\|\|\kappa_e\|\|$ (m)	0.35/0.14	22.2/9.94	0.46/0.13	0.45/0.15
min $\|\|\tau_e\|\|$ (m)	0.0209	0.3251	0.1335	0.0072
max $\|\|\tau_e\|\|$ (m)	5.3908	17.7734	4.7620	4.8905
mean $\|\|\tau_e\|\|$ (m)	1.9622	6.8107	2.9828	2.9577
Observability score	17.234	6.5732	15.6987	15.3195

Simulations with the gliding robotic fish are carried out in a similar fashion to that of the unicycle. We leverage the tracking controller developed in [29] as the baseline controller with a 5 Hz control rate. The controller requires a reference trajectories for the pitch angle and Cartesian position. The pitch refeference is a constant that changes sign when a depth threshold is hit, the position references are provided by the target, and the z position reference is given as the current depth of the gliding robotic fish.

Figure 2 shows the resultant trajectories produced by the baseline controller with and without the control barrier function. Again, for each control approach, two cases, with and without the relative position measurement, are simulated. Under state feedback, tracking is achieved with and without the control barrier function. When the CBF is not present, the robot follows the target closely during the beginning and end of the trajectory, but veers from the target path near the middle. When the tracking controller is modified by the CBF, the robot initially follows the target path more loosely. When tracking is based on the EKF position estimates, the tracking is unsuccessful without the CBF. When it is present, a trajectory similar to the state feedback case with the CBF is produced.

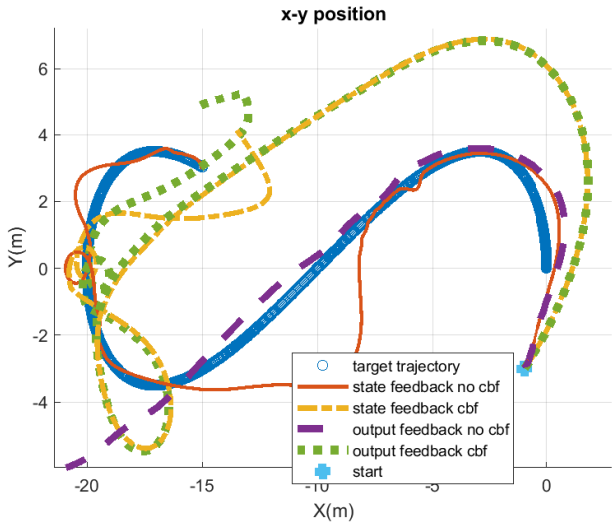

Fig. 2. $x - y$ plane projections of paths generated from gliding robotic fish tracking a target moving in a figure-8 pattern using the baseline tracking controller with and without the control barrier function in the case of state and output feedback on position.

The statistics taken over the resultant trajectories, shown in Table II, quantify the behavior of each of the 4 scenarios. As expected, the observability score is lowest, and the max tracking error norm, and the max estimation error norm are highest for the output feedback case when the control barrier function is not applied. When the output feedback controller is integrated with the CBF, statistics for the estimation and tracking error norms and observability score are similar to those of the state feedback controller with the CBF. When the CBF is not present in the state feedback controller, the mean tracking and estimation error norms are lowest of the 4 scenarios. The observability score is also higher, but this is expected because it has been shown that the inverse condition number for the observability matrix of the range measurement degrades as range increases [12].

E. Comparison Between Constraint-Based and Optimization Based Approaches

In our previous work [18], we addressed target tracking with range only measurement by posing and solving the

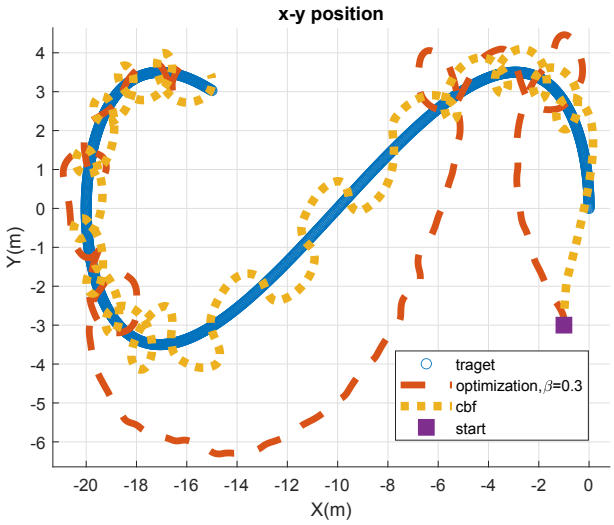

Fig. 3. Paths generated from a unicycle tracking a target moving in a figure-8 pattern with control barrier funtion-based and observability optimization-based controllers.

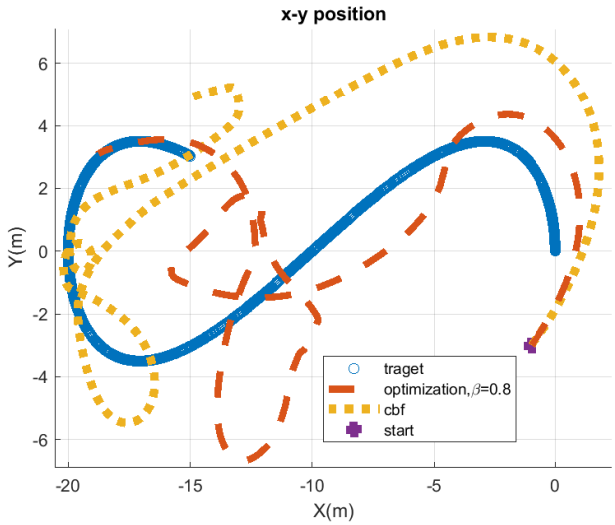

Fig. 4. $x-y$ plane projection of paths generated from gliding robotic fish tracking a target moving in a figure-8 pattern with control barrier funtion-based and observability optimization-based controllers.

optimization problem

$$\begin{aligned} \min_{u} \quad & J = \int_{T_0}^{T_1} \beta||\tau_e||^2 + (1-\beta)O dt \\ & \text{subject to the dynamics (11),} \\ & u_{min} \leq u \leq u_{max} \end{aligned} \tag{23}$$

over a finite time horizon, where β is a tuning parameter to be chosen and O is some observability metric. This work leverages the control barrier function framework discussed in Section II-B to enforce observability in a point wise fashion. The two approaches are compared using $O = -B(X_c)$ for the output feedback case for the unicycle model in Fig. 3 and the gliding robotic fish model in Fig. 4. For the unicycle, it is clear to see that the control barrier function-based approach is superior with respect to the tracking objective. Table III shows that CBF-based approach performs better on all metrics. For the gliding robotic fish model, both methods are only able to loosely track the target, but Table III shows the CBF-based approach to have the advantage. It also has a slight advantage in terms of tracking and estimation error.

TABLE III
OPTIMIZATION VS CONSTRAINT BASED APPROACHES: STATISTICS AND OBSERVABILITY SCORE

method	Optimze	CBF	Optimize	CBF
sysyem	unicycle	unicycle	glider	glider
max/mean $\|\|\kappa_e\|\|$ (m)	1.30/0.33	0.52/0.12	0.62/0.19	0.45/0.15
min $\|\|\tau_e\|\|$ (m)	0.0166	0.0317	0.0722	0.0072
max $\|\|\tau_e\|\|$ (m)	4.1965	3.1623	9.0728	4.8905
mean $\|\|\tau_e\|\|$ (m)	1.6762	0.7528	4.0742	2.9577
Observability Score	39.6335	74.589	13.9230	15.3195

One difference in the two approaches is that the solution to (23) directly gives a set of controls that jointly maximizes $B(X_c)$ and minimizes $||\tau_e||$ over the time horizon T_0 to T_1, while the approach taken in this paper modifies the control of a nominal controller in order to satisfy the nonlinear observability rank condition discussed in II-A. The major advantages of the control barrier function-based approach are provable forward invariance, relative ease of computation for control affine systems, and no requirement for the tuning parameter β that gives a relative importance to the control objective versus maintaining observability. Instead of giving the choice of the tradeoff in the control design, the proposed approach guarantees that the system remains observable and makes progress toward the tracking objective whenever possible. In terms of computation, the CBF-based approach is much less intensive. The time to simulate the 250 second trajectory for the CBF-based approach is approximately 75% of the time required for the optimization based approach with the unicycle model and 5% with the gliding robotic fish model. In addition, it requires no prediction or future knowledge of the target trajectory.

In [18], the optimization-based approach was also used with two other metrics, the inverse condition number and the posterior probability of the estimation error, to improve the estimation error. The latter is dependent on the estimation scheme and does not immediately present a way to define a set that enforces observability. The inverse condition number itself, however, can be used as a zeroing barrier function. Like the determinant, the inverse condition number provides a straight forward constraint for enforcing observability and is a property of the observability matrix, so increasing it improves estimation regardless of the estimation scheme. However, the expression for the inverse condition number is not as simple as the determinant, but would likely produce the same set of valid controls.

V. Conclusion and Future Work

In this work, we studied the use of control barrier functions to improve observability and enhance overall control performance for a mobile robot in target tracking with only distance measurements. By introducing a barrier function based on an observability metric, an observable set that satisfied the nonlinear observability rank test was formed. Forward invariance of that set was enforced through the minimally invasive controller formulation used in the control barrier function literature. Simulation studies were carried out for a unicycle model and a gliding robotic fish model. The example systems were shown to improve observability (in terms of the inverse condition number) and estimation performance, enabling tracking without access to the relative position to the target. The results were compared to an optimization-based solution for the same objective and shown to be better overall in terms of tracking performance and estimation error. While this paper focuses mainly on the application of target tracking given range measurements, enforcing observability through control barrier functions (observability barrier functions) may be applicable to other types of systems.

Future directions for this work include thorough analysis of forward invariance subject to output feedback, exploration of a barrier function based on the estimator's error covariance, and evaluation of this method on physical systems.

References

[1] J. Wu, R. C. Bingham, S. Ting, K. Yager, Z. J. Wood, T. Gambin, and C. M. Clark, "Multi-AUV motion planning for archeological site mapping and photogrammetric reconstruction," *Journal of Field Robotics*, vol. 36, no. 7, pp. 1250–1269, 2019.

[2] S. B. Williams, O. Pizarro, M. Jakuba, and N. Barrett, "AUV benthic habitat mapping in South Eastern Tasmania," in *Field and Service Robotics*. Springer, 2010, pp. 275–284.

[3] L. Paull, S. Saeedi, M. Seto, and H. Li, "AUV navigation and localization: A review," *IEEE Journal of Oceanic Engineering*, vol. 39, no. 1, pp. 131–149, 2013.

[4] "Woods Hole Oceanographic Instituttion: Acoustic Micromodem," https://acomms.whoi.edu/micro-modem/, 2021.

[5] A. S. Gadre and D. J. Stilwell, "A complete solution to underwater navigation in the presence of unknown currents based on range measurements from a single location," in *2005 IEEE/RSJ International Conference on Intelligent Robots and Systems*. IEEE, 2005, pp. 1420–1425.

[6] Q. Chen, K. You, and S. Song, "Cooperative localization for autonomous underwater vehicles using parallel projection," in *2017 13th IEEE International Conference on Control & Automation (ICCA)*. IEEE, 2017, pp. 788–793.

[7] A. Bahr, J. J. Leonard, and M. F. Fallon, "Cooperative localization for autonomous underwater vehicles," *The International Journal of Robotics Research*, vol. 28, no. 6, pp. 714–728, 2009.

[8] Y. Huang, Y. Zhang, B. Xu, Z. Wu, and J. A. Chambers, "A new adaptive extended Kalman filter for cooperative localization," *IEEE Transactions on Aerospace and Electronic Systems*, vol. 54, no. 1, pp. 353–368, 2017.

[9] M. F. Fallon, G. Papadopoulos, J. J. Leonard, and N. M. Patrikalakis, "Cooperative AUV navigation using a single maneuvering surface craft," *The International Journal of Robotics Research*, vol. 29, no. 12, pp. 1461–1474, 2010.

[10] P. Baccou and B. Jouvencel, "Homing and navigation using one transponder for AUV, postprocessing comparisons results with long base-line navigation," in *Proceedings 2002 IEEE International Conference on Robotics and Automation (Cat. No. 02CH37292)*, vol. 4. IEEE, 2002, pp. 4004–4009.

[11] A. Ross and J. Jouffroy, "Remarks on the observability of single beacon underwater navigation," in *Proc. Intl. Symp. Unmanned Unteth. Subm. Tech*, 2005.

[12] F. Arrichiello, G. Antonelli, A. P. Aguiar, and A. Pascoal, "An observability metric for underwater vehicle localization using range measurements," *Sensors*, vol. 13, no. 12, pp. 16 191–16 215, 2013.

[13] B. T. Hinson, M. K. Binder, and K. A. Morgansen, "Path planning to optimize observability in a planar uniform flow field," in *2013 American Control Conference*. IEEE, 2013, pp. 1392–1399.

[14] G. Antonelli, F. Arrichiello, S. Chiaverini, and G. S. Sukhatme, "Observability analysis of relative localization for AUVs based on ranging and depth measurements," in *2010 IEEE International Conference on Robotics and Automation*. IEEE, 2010, pp. 4276–4281.

[15] M. Rafieisakhaei, S. Chakravorty, and P. Kumar, "On the use of the observability gramian for partially observed robotic path planning problems," in *2017 IEEE 56th Annual Conference on Decision and Control (CDC)*. IEEE, 2017, pp. 1523–1528.

[16] B. Ferreira, A. Matos, and N. Cruz, "Single beacon navigation: Localization and control of the MARES AUV," in *OCEANS 2010 MTS/IEEE SEATTLE*. IEEE, 2010, pp. 1–9.

[17] J. D. Quenzer and K. A. Morgansen, "Observability based control in range-only underwater vehicle localization," in *2014 American Control Conference*. IEEE, 2014, pp. 4702–4707.

[18] D. Coleman, S. Bopardikar, and X. Tan, "Observability-aware target tracking with range only measuremeants," in *2021 American Control Conference (ACC)*. IEEE, 2021.

[19] A. D. Ames, J. W. Grizzle, and P. Tabuada, "Control barrier function based quadratic programs with application to adaptive cruise control," in *53rd IEEE Conference on Decision and Control*. IEEE, 2014, pp. 6271–6278.

[20] U. Borrmann, L. Wang, A. D. Ames, and M. Egerstedt, "Control barrier certificates for safe swarm behavior," *IFAC-PapersOnLine*, vol. 48, no. 27, pp. 68–73, 2015.

[21] A. D. Ames, X. Xu, J. W. Grizzle, and P. Tabuada, "Control barrier function based quadratic programs for safety critical systems," *IEEE Transactions on Automatic Control*, vol. 62, no. 8, pp. 3861–3876, 2016.

[22] A. D. Ames, S. Coogan, M. Egerstedt, G. Notomista, K. Sreenath, and P. Tabuada, "Control barrier functions: Theory and applications," in *2019 18th European Control Conference (ECC)*. IEEE, 2019, pp. 3420–3431.

[23] D. Panagou, D. M. Stipanovič, and P. G. Voulgaris, "Multi-objective control for multi-agent systems using lyapunov-like barrier functions," in *52nd IEEE Conference on Decision and Control*. IEEE, 2013, pp. 1478–1483.

[24] D. Panagou, D. M. Stipanović, and P. G. Voulgaris, "Distributed coordination control for multi-robot networks using lyapunov-like barrier functions," *IEEE Transactions on Automatic Control*, vol. 61, no. 3, pp. 617–632, 2015.

[25] L. Wang, A. D. Ames, and M. Egerstedt, "Multi-objective compositions for collision-free connectivity maintenance in teams of mobile robots," in *2016 IEEE 55th Conference on Decision and Control (CDC)*. IEEE, 2016, pp. 2659–2664.

[26] P. Glotfelter, J. Cortés, and M. Egerstedt, "Nonsmooth barrier functions with applications to multi-robot systems," *IEEE control systems letters*, vol. 1, no. 2, pp. 310–315, 2017.

[27] R. Hermann and A. Krener, "Nonlinear controllability and observability," *IEEE Transactions on Automatic Control*, vol. 22, no. 5, pp. 728–740, 1977.

[28] F. Zhang, "Modeling, design and control of gliding robotic fish," Dissertation, Michigan State University. Electrical Engineering, 2014.

[29] D. Coleman and X. Tan, "Backstepping control of gliding robotic fish for trajectory tracking in 3D space," in *2020 American Control Conference (ACC)*. IEEE, 2020, pp. 3730–3736.